ACI MATERIALS JOURNAL TECHNICAL PAPER

Title no. 107-M35

Assessing Mechanical Properties and Microstructure of Fire-Damaged Engineered Cementitious Composites

by Mustafa Sahmaran, Mohamed Lachemi, and Victor C. Li

In the last few years, a number of investigations of engineered cementitious composites (ECC) have been carried out, and the mechanical behavior and durability characteristics of this type of composite are now increasingly better understood. The fire-resistant behavior of this specialized concrete, however, has not yet been studied as extensively. This investigation develops important data on the mechanical properties and microstructure of ECC exposed to temperatures up to 800°C (1472°F). In this study, the mechanical properties (the residual compressive strength, stress-strain curve, and stiffness) and mass loss were determined after air cooling, subsequent to temperature exposure. Changes in the microstructure, porosity, and pore size distribution of the fire-deteriorated ECC specimens were identified using scanning electron microscopy (SEM) and mercury intrusion porosimetry (MIP) techniques. Test results revealed no significant changes in the mechanical properties for tested specimens exposed to temperatures up to 400°C (752°F) for an hour. Microstructural analysis showed the creation of supplementary pores and channels in the matrix due to polyvinyl alcohol (PVA) fibers melting in the 200 to 400°C (392 to 752°F) temperature range. After a 1-hour exposure to temperatures of 600 and 800°C (1112 and 1472°F), the mechanical performance of fire-deteriorated ECC mixture is similar to or better than that of conventional concrete incorporating polypropylene or steel fibers, despite a significant reduction in compressive strength and stiffness. Moreover, no explosive spalling occurred in any specimens during the fire test. The promising performance of ECC under fire exposure may be due to the presence of PVA fibers and high-volume fly ash (FA). The beneficial influence of FA can be ascribed to the pozzolanic reaction consuming calcium hydroxide in the hydrates. PVA fiber is also beneficial in that it prevents explosive spalling. This introduces additional channels for vaporized moisture in ECC to escape without creating high internal pressure in the material.

Keywords: compressive strength; engineered cementitious composites; fire resistance; microstructure; stiffness.

INTRODUCTION

An engineered cementitious composite (ECC) is a newly developed, high-performance fiber-reinforced cementitious composite with substantial benefits; it offers high ductility under uniaxial tensile loading and improved durability due to an intrinsically tight crack width of less than 100 μm (0.004 in.). This tight crack width is self-controlled and, whether the composite is used in combination with conventional reinforcement or not, it is a material characteristic independent of the number and size of reinforcing bars.[1,2] Tight crack width is as important to the durability of ECC structures as tensile ductility is to structural safety at an ultimate limit state.[3-9] Under severe bending load, an ECC beam deforms similarly to a ductile metal plate through plastic deformation. Under compression, ECC materials exhibit compressive strengths that are similar to high-strength concrete (for example, greater than 60 MPa [8.7 ksi]).[10] As a result of these excellent properties, the use of ECC has become increasingly popular over the last few years. Its versatility is also a significant benefit; ECC can be used in a variety of structures, such as high-rise buildings, bridges, tunnels, highways, and other forms of infrastructures.[11,12]

Although various fiber types have been used in the production of ECC, PVA fiber was adopted in the current version based on composite performance and economic consideration. At present, PVA-ECC represents the most practical ECC used in the field.[11-12] To account for material inhomogeneity, a fiber content of 2% by volume in excess of the calculated critical fiber content has been typically used in the mixture design. The choice to use the PVA fiber in this study is based on the fact that it has been shown to produce good ECC properties (tight crack width and high tensile ductility) in previous laboratory and field investigations.[11-14]

With an increase in the application of ECC, the risk of exposure to elevated temperatures increases as well. For normal concrete, high temperatures cause physical and chemical changes, resulting in its mechanical property deterioration, such as compressive strength and modulus of elasticity. The spalling of concrete under high temperatures is a concern due to the exposure of the steel reinforcement to direct fire contact and a subsequent structural capacity loss of the element. The most commonly used solution, besides mixture proportioning, is adding low melting-point synthetic (mostly polypropylene [PP]) fibers. In case of high temperature exposure, not all water is expelled fast enough from the concrete with a very dense internal structure. The inclusion of PP fibers reduces the likelihood of concrete spalling at high temperatures because water vapor can exit through channels created by the melted fibers.[15-22] When the PP fiber concrete with dense internal structure is heated up to approximately 170°C (338°F), the fibers readily melt and volatilize, creating additional pores and small channels in the concrete that may act to relieve high internal vapor pressures and reduce the likelihood of spalling.[22]

PVA synthetic fibers in ECC may behave similarly to PP fibers; they may also melt and leave sufficient space for steam to escape, thereby avoiding internal pressure build-up and associated cover bursting. So far, no experimental data on the fire resistance of ECC has been published. This investigation contributes to the understanding of ECC performance under high temperatures. To predict the response of ECC structures during and after exposure to elevated temperatures, it is essential

ACI Materials Journal, V. 107, No. 3, May-June 2010.
MS No. M-2009-217 received June 22, 2009, and reviewed under Institute publication policies. Pertinent discussion including authors' closure, if any, will be published in the March-April 2011 *ACI Materials Journal* if the discussion is received by December 1, 2010.

ACI member **Mustafa Sahmaran** *is an Assistant Professor in the Department of Civil Engineering at the University of Gaziantep, Southeastern Anatolia, Turkey. He is a member of ACI Committee 237, Self-Consolidating Concrete. His research interests include concrete technology, durability of concrete, and composite materials development for sustainable infrastructure.*

ACI member **Mohamed Lachemi** *is a Canada Research Chair in Sustainable Construction and a Professor in the Department of Civil Engineering at Ryerson University, Toronto, ON, Canada. He is a member of ACI Committees 231, Properties of Concrete at Early Ages, and 237, Self-Consolidating Concrete. His research interests include the use of high-performance materials in the built infrastructure, including the development and use of self-consolidating concrete in construction.*

ACI member **Victor C. Li** *is a Professor in the Department of Civil and Environmental Engineering at the University of Michigan, Ann Arbor, MI. He is a member of ACI Committee 544, Fiber Reinforced Concrete. His research interests include the design of ultra-ductile and green cementitious composites, their application to innovative infrastructure systems, and integration of materials and structural design.*

Table 1—Mixture proportions of ECC

	ECC (M45)
FA/C	1.2
w/cm	0.27
Water (W), kg/m^3 (lb/yd^3)	326 (549)
Cement (C), kg/m^3 (lb/yd^3)	558 (940)
Fly ash (FA), kg/m^3 (lb/yd^3)	669 (1127)
Cementitious materials, kg/m^3 (lb/yd^3)	1227 (2067)
Sand (S), kg/m^3 (lb/yd^3)	446 (751)
Fiber, kg/m^3 (lb/yd^3)	26 (44)
WRA, kg/m^3 (lb/yd^3)	2.30 (3.9)
28-day uniaxial tensile strength, MPa (ksi)	5.1 (0.74 ksi)
28-day uniaxial tensile strain, %	2.7

Table 2—Chemical composition and physical properties of cement and fly ash

Chemical composition, %	Cement	Fly ash
CaO	61.80	5.57
SiO_2	19.40	59.50
Al_2O_3	5.30	22.20
Fe_2O_3	2.30	3.90
MgO	0.95	—
SO_3	3.80	0.19
K_2O	1.10	1.11
Na_2O	0.20	2.75
Loss on ignition	2.10	0.21
Physical properties		
Specific gravity	3.15	2.18
Retained on 45 μm (0.002 in.), %	12.9	9.6
Water requirement, %	—	93.4

to gain a clear understanding of the microstructural and mechanical properties of ECC subjected to those conditions.

This paper gives the results of an investigation on the performance of ECC material under fire exposure. For this study, a standard ECC mixture (M45) was prepared and exposed to temperatures up to 800°C (1472°F). Residual mechanical properties including compressive strength, stress-strain curve, and stiffness were measured. To gain insight into residual properties, pore size distribution was also determined by the mercury intrusion porosimetry (MIP) technique. Microstructural changes within the matrix were analyzed using scanning electron microscopy.

Table 3—Characteristics of PVA fiber

Fibers	PVA
Nominal strength, MPa (ksi)	1620 (235)
Apparent strength, MPa (ksi)	1092 (158)
Diameter, μm (in.)	39 (0.002)
Length, mm (in.)	8 (0.3)
Young's modulus, GPa (ksi)	42.8 (6200)
Elongation, %	6.0
Density, kg/m^3 (lb/yd^3)	1300 (2190)
Melting temperature, °C (°F)	230 (446)

RESEARCH SIGNIFICANCE

ECC is a relatively new material, with a number of benefits, including high ductility under uniaxial tensile loading and improved durability due to an intrinsically tight crack width. A greater understanding of its behavior under different conditions will improve confidence in its use. Determining the fire performance of ECC is critical due to its use in high-rise buildings and tunnel structures. This research adds important data to existing information on the behavior of ECC under elevated temperatures. Because ECC contains PVA fiber and more powder-like constituents than conventional concrete, it is not known a priori whether the fire resistance of ECC is the same as conventional concrete. Understanding the ability of PVA fibers to prevent spalling is critical to the design and construction of safe and durable structures.

EXPERIMENTAL STUDIES

Materials, mixture proportions, and basic mechanical properties

An experimental program was designed to investigate the residual mechanical and microstructural properties of ECC after exposure to elevated temperatures. For this purpose, a standard ECC mixture (M45) with a fly ash-cement ratio (FA/PC) of 1.2 by mass was prepared, details of which are provided in Table 1. The components of ECC mixtures are similar to typical fiber-reinforced cement composites (FRCC), consisting of Type I portland cement (PC), sand, Class F fly ash (FA), water, fibers, and a water-reducing admixture (WRA). The chemical composition and physical properties of cement and FA are presented in Table 2. Unlike typical FRCCs, however, the component characteristics and proportions within the ECC are carefully determined with the use of micromechanical design tools to achieve the desired strain-hardening response.[23] To minimize the mortar matrix fracture toughness, no large aggregates were used, and the silica sand had an average grain size of 110 μm (0.004 in.) and a maximum size of 200 μm (0.008 in.). The PVA fibers were manufactured with a tensile strength, elastic modulus, and a maximum elongation matching those needed for strain-hardening performance. Additionally, the surface of the PVA fibers was coated with a proprietary hydrophobic oiling agent of 1.2% by weight to control the interfacial bonding properties between the fiber and matrix for strain-hardening performance.[23] The mechanical, geometrical, and thermal properties of the PVA fibers used in this study are shown in Table 3. The melting temperature of PVA fibers was 230°C (446°F).

The ultimate tensile strain capacity of the ECC mixture at 28 days is listed in Table 1. To characterize the direct tensile behavior of the ECC mixtures, 200 x 75 x 13 mm (8.0 x 3.0 x 0.5 in.) coupon specimens were used. Direct tensile tests were conducted under displacement control at a loading rate

of 0.005 mm/second (0.0002 in./second). The typical tensile stress-strain curves of the ECC mixture at 28 days are shown in Fig. 1. After first cracking, the uniaxial tensile stress increased at a slower rate, along with the development of multiple cracks with a small crack spacing and tight crack widths. As seen in Table 1, the ECC composite exhibited a strain capacity of 2.7% at 28 days. After direct tensile testing, all residual crack widths were also measured in the unloaded stage on the surface of the specimens using a portable microscope. All of the ECC coupon specimens showed multiple cracking behaviors with small crack spacing and tight crack widths (<70 μm [0.003 in.]).

TEST SPECIMEN PREPARATION AND TESTING

Several 50 mm (2 in.) cubes were cast to determine the residual mechanical and microstructural properties. After removal from the molds at 1 day, the specimens were conditioned in an environmental chamber at a temperature of 23 ± 2°C (73°F) and a relative humidity of 95 ± 5% until the age of 28 days. Six cubes were tested under compression immediately after conditioning; these control specimens will be referred to as those tested after exposure to the normal curing condition (unheated). The remaining specimens were heated to targeted temperatures at the age of 28 days, and their residual properties were then investigated. The heating equipment used in the investigation was a computer-controlled, electrically heated furnace. In the furnace, the cubes were heated at a constant rate of approximately 15°C/minute (59°F/minute) to reach the prescribed temperatures. Four maximum temperatures (200, 400, 600, and 800°C [392, 752, 1112, and 1472°F]) were chosen. When the targeted peak temperature was reached, the furnace temperature was maintained constant for 60 minutes to achieve the thermal steady state.[24] After that, the samples were allowed to cool naturally to room temperature.

After the cooling period, the compression strength tests were carried out on the cubes, including control samples not exposed to high temperatures. An axial load test was performed under displacement control at a loading rate of 0.005 mm/second (0.0002 in./second) on a closed-loop controlled servo-hydraulic material test system with 200 kN (45 kip) capacity. During the compressive tests, the load and the deflection values were recorded on a computerized data recording system. Six specimens were tested for each stage and average values were recorded. The weight of each specimen was also measured before and after exposure to calculate the mass loss of fire-deteriorated specimens.

MIP was used to characterize the pore size distribution before and after exposure to high temperatures. An instrument capable of producing pressures up to 414 MPa (60 ksi) and assuming a contact angle of 130 degrees was used for pore size distribution analysis. Prior to testing, specimens were dried to a constant weight at 50°C (122°F). In all cases, at least two identical ECC specimens were tested at the same time. The microstructure of both specimens was also analyzed using scanning electron microscopy.

RESULTS AND DISCUSSIONS

Microstructural properties

It is generally accepted that the mechanical properties of any material are closely linked to its microstructure. The microstructure controls water release from concrete at both normal and elevated temperatures. Thus, to a certain degree, the variation in microstructure reflects the deterioration of

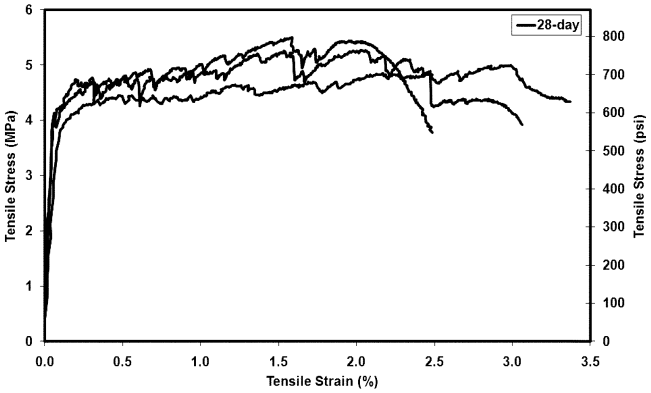

Fig. 1—Typical tensile stress-strain response of standard ECC mixture (M45).

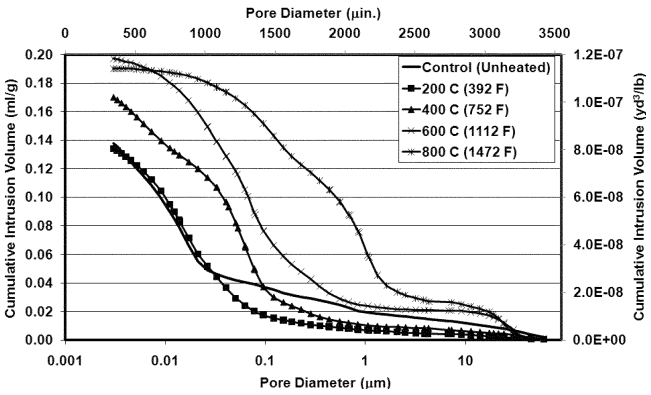

Fig. 2—Pore size distributions of ECC before and after exposure to high temperatures.

materials subjected to high temperatures. In this study, MIP tests and scanning electron microscopy (SEM) were used to identify the changes in the microstructure, porosity and pore size distribution of fire-deteriorated hardened ECC specimens.

Porosity and average pore size measurements

The porosity and average pore size of ECC control (unheated) specimens and specimens subjected to various elevated temperatures were measured using a mercury intrusion porosimetry test. MIP is a well-developed technique that can provide information about pore structure, including the porosity, average pore diameter, and pore size distribution of ECC. Figure 2 provides the variations of cumulative pore volume and its distribution as influenced by different heating regimes. The deterioration of ECC's structural integrity, when exposed to various temperatures, is illustrated by an average pore diameter and total intruded porosity increase in Table 4. As seen in Table 4, the higher the temperature, the coarser the pore structure, and the higher the total intruded porosity of ECC. The total intruded porosity only increased by approximately 0.2% after exposure to 200°C (392°F), with an insignificant change in average pore diameter. Porosity increased by approximately 5% after exposure to 400°C (752°F), and by approximately 9% for 600 and 800°C (1112 and 1472°F). In terms of total intruded porosity and coarsening (average pore diameter), the changes appeared more rapidly with temperatures over 600°C (1112°F). Therefore, the average pore diameter dramatically enlarged three to ten times its original size after ECC had been exposed to 600 and 800°C (1112 and 1472°F), respectively.

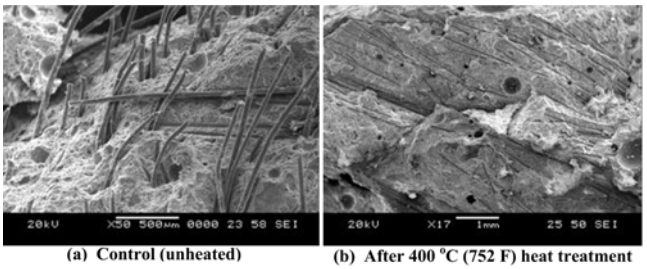

(a) Control (unheated) (b) After 400 °C (752 F) heat treatment

Fig. 3—SEM micrograph of ECC before and after thermal treatment.

Table 4—Total intruded porosity and average pore diameter of ECC samples

Specimen		ECC (M45)
Control (unheated)	Total intruded porosity, %	23.7
	Average pore diameter, nm (μin.)	12.1 (0.48)
200°C (392°F)	Total intruded porosity, %	23.9
	Average pore diameter, nm (μin.)	13.4 (0.53)
400°C (752°F)	Total intruded porosity, %	28.6
	Average pore diameter, nm (μin.)	18.2 (0.72)
600°C (1112°F)	Total intruded porosity, %	32.0
	Average pore diameter, nm (μin.)	31.9 (1.26)
800°C (1472°F)	Total intruded porosity, %	32.4
	Average pore diameter, nm (μin.)	113.6 (4.47)

The MIP test results highlight pore structure coarsening and the increase in porosity at elevated temperatures; these are the major reasons for the strength and stiffness losses (to be discussed in the following sections). In ECC, the pore structure coarsening effect was more pronounced at temperatures over 600°C (1112°F). After an exposure up to 400°C (752°F), the MIP test results given in Fig. 2 indicate that the ECC showed reduction in the cumulative volume of pores larger than 0.1 μm (3.94 μin.), which generally influences the strength of the concrete.[25] The reduction of the cumulative volume of pores larger than 0.1 μm (3.94 μin.) may be due to the further hydration of unhydrated cement particles and the pozzolanic reaction of FA particles with free lime to produce more C-S-H phases deposited in the pore system.[26] Because the coarsening of ECC was not significant in this temperature range, the strength and stiffness loss occurred at temperatures up to 400°C (752°F) can be attributed to internal cracking. This was probably due to the very dense internal structure of ECC, which results in an increased vapor pressure formed by the evaporation of free physically bound water. As seen from Fig. 2, the cumulative volume of pores larger than 0.1 μm (3.94 μin.) greatly increased after exposure to temperatures of 600°C (1112°F) and above. The degradation of hydrates (C-S-H gels), which is inevitable when the exposure temperature is raised to 600°C (1112°F)[27] and above, is the main reason for severe pore structure coarsening.

SEM observations

To study the behavior of fibers and matrix microstructure after exposure to several peak temperature levels, observations with an SEM were performed on samples taken from the cores of 50 cm (2 in.) ECC specimens exposed to temperatures of 200, 400, 600, and 800°C (392, 752, 1112, and 1472°F) for 1 hour. Figure 3(a) shows a general view of PVA fibers

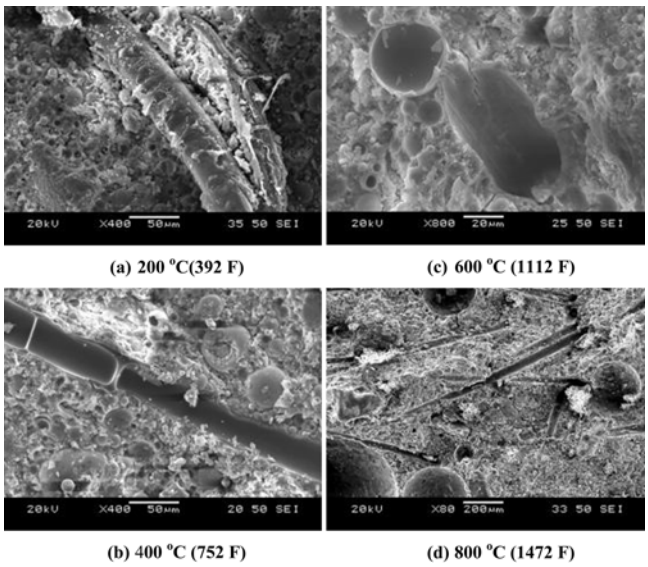

(a) 200 °C(392 F) (c) 600 °C (1112 F)

(b) 400 °C (752 F) (d) 800 °C (1472 F)

Fig. 4—SEM micrograph of ECC after subjected to various temperatures.

scattered in an unheated ECC control specimen. Micrographs of the unheated samples mainly consisted of ill-crystallized and fibrous particles of C-S-H gel, amorphous and well-crystallized calcium hydroxide, and numerous unhydrated FA particles. Figure 3(b) shows the SEM micrograph of heated ECC specimens at 400°C (752°F). The SEM micrograph showed multiple small channels created in the ECC due to PVA fiber melting.

Figure 4 shows closer-view SEM micrographs of thermally-treated ECC specimens at various temperatures. Figure 4(a) shows that the microstructure of the ECC specimen did not undergo changes and did not suffer any apparent cracking after fire exposure at 200°C (392°F). At 400°C (752°F), PVA fibers melt completely, increasing the total intruded porosity of the matrix and creating additional interconnected pores and small channels in the matrix that can decrease pore pressure inside the ECC (Fig. 4(b)). As seen in Fig. 3(b), the fiber content is high enough that fibers alone constitute a connected network. Therefore, the use of PVA fiber clearly affects porosity at high temperatures. After exposure to 600 and 800°C (1112 and 1472°F), the morphology of hydration products showed a massive structure; almost all of them lost their characteristic crystalline appearance showing an ill-crystallized or amorphous structure (Fig. 4(c) and (d)). The SEM analysis also indicated that beyond 800°C (1472°F), microcracking increased around the grains of unhydrated FA particles.

Mass loss and surface characteristics

The deterioration of specimens subjected to various elevated temperatures was also assessed by mass loss measurements. Figure 5(a) shows the relation between mass loss (M_i/M_0) (in percentage) and temperature of heat-exposed ECC. M_i is the mass after a specific thermal heat exposure, and M_0 is initial mass, prior to heat exposure. As seen in Fig. 5(a), the mass loss increased with the increasing temperature of thermal exposure, a result mainly associated with the liberation of free and physically bound water. At higher temperatures of 600 and 800°C (1112 and 1472°F), the weight change of ECC was caused by the dehydration of paste as discussed in the preceding section. During a heat treatment up to 400°C

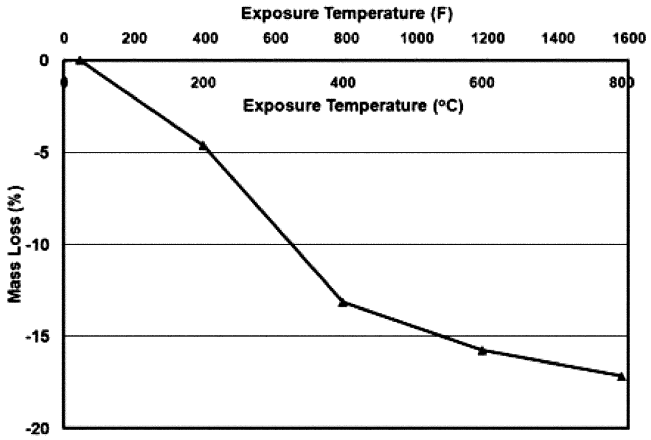

(a) Mass loss

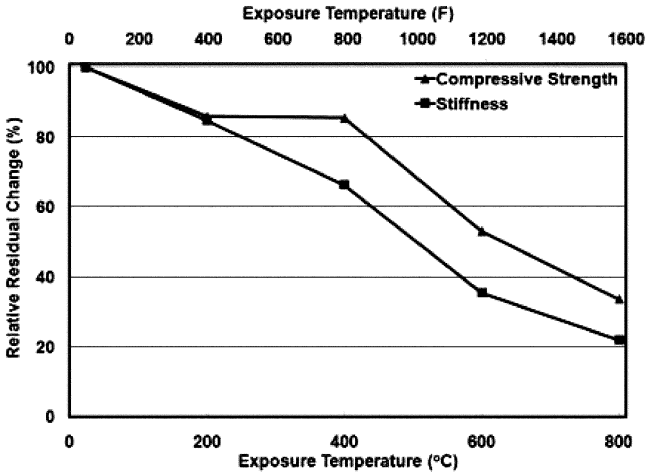

(b) Compressive strength and stiffness

Fig. 5—Degradation of ECC in terms of: (a) mass loss; and (b) compressive strength and stiffness as function of exposure temperature.

(752°F), the weight of the melted fibers also had an influence on mass loss.

Figure 6 shows surface crack patterns of ECC specimens as a result of various elevated temperatures. Cracking became apparent when the exposure temperatures exceeded 400°C (752°F). In some of the cubes, hairline cracks were observed at 400°C (752°F) (Fig. 6(b)). At temperatures above 400°C (752°F), microcracking increased significantly (Fig. 6(c) and (d)), first around hydration products and then around grains of unhydrated FA and cement.

Thermal explosive spalling is a catastrophic failure of concrete that generally occurs during a fire and is characterized by the explosive fracture and ejection of pieces of the material, often without prior warning. The phenomenon is not fully understood, especially for high-performance concrete. For example, spalling is not consistently observed, even for specimens tested under identical conditions.[28] Despite this inconsistency, it is believed that spalling occurs under a specific combination of test conditions. From a mechanics perspective, spalling is a result of nonuniformity of stress distribution in a material.[28] Previous studies demonstrated that spalling in concrete occurs between 190 and 250°C (374 and 482°F).[22] In this study, no spalling and splitting/cracking were observed after the ECC specimens were subjected to air cooling after being exposed to peak

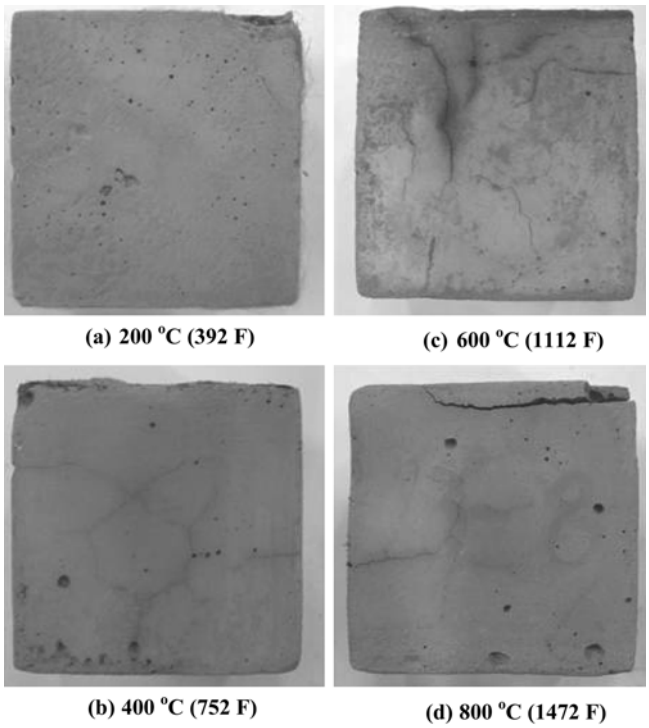

Fig. 6—Typical crack patterns on surface of ECC specimens after exposure to high temperatures.

Table 5—Effect of temperature on compressive strength and relative stiffness

Specimen	Compressive strength, MPa (ksi)	Relative stiffness, %
Control (unheated)	64.3 (9.33) [3.2 (0.46)]	100
200°C (392°F)	55.2 (8.00) [4.4 (0.64)]	84.7
400°C (752°F)	54.9 (7.96) [2.5 (0.36)]	66.3
600°C (1112°F)	34.2 (4.96) [1.4 (0.20)]	35.5
800°C (1472°F)	21.6 (3.13) [1.2 (0.17)]	21.9

Note: Numbers in brackets are standard deviations in MPa (ksi).

temperatures of up to 800°C (1472°F). This result indicates that the path of moisture escape created after the melting of PVA fibers had a significant influence on suppressing surface spalling.

Compressive strength, stiffness, and stress-strain curve

To predict the behavior of structures employing ECC after exposure to elevated temperatures, the compressive strength of test specimens was measured shortly after heating, when specimens had cooled to room temperature. Table 5 summarizes the compression strength results for specimens cured normally (unheated) and tested after exposure to elevated temperatures. In the table, each value represents the average result of at least five specimens. Complete stress-strain curves of both the unheated and heated specimens were also obtained from compression tests, performed with a displacement control rate of 0.005 mm/second (0.0002 in./second) on a closed-loop controlled servo-hydraulic material test system. The typical compressive behavior of the tested specimens is presented in Fig. 7. It should be noted that the axial strains of concrete in compression were obtained from full-height shortening of the cubic

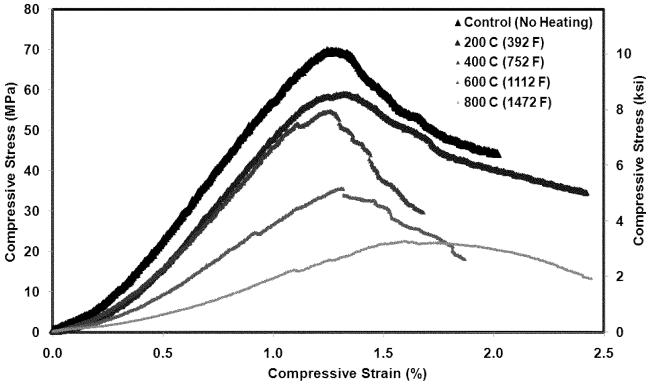

Fig. 7—Effect of elevated temperatures on compressive stress-strain curves of ECC.

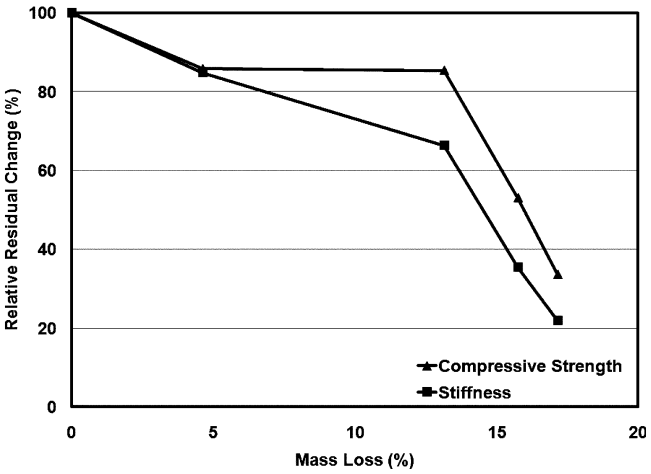

Fig. 8—Correlation between percentage residual stiffness and compressive strength versus percentage mass loss.

specimens using linear variable displacement transducers (LVDTs). Such strains are generally larger than those obtained at the midheight region due to the end effects.[29] The typical compressive stress-strain curves of ECC specimens after thermal deterioration show that the influence of elevated temperatures up to 400°C (752°F) on compressive properties is fairly minor (Fig. 7). This result is consistent with the results of the microstructural analysis of ECC specimens reported previously (Table 4).

Figure 7 shows that the material stiffness (slope of the load-deflection curve of the ECC cubic specimens) decreases with an increase in exposure temperature up to 800°C (1472°F). The figure also shows that after exposure to elevated temperatures, the initial ascending parts of the curve for the ECC were approximately linear, but the stiffness magnitudes were much lower. The decrease in stiffness (in percentage) with increasing temperature is summarized in Table 5, where the ECC stiffness data were obtained within 30% of the ultimate strength and were given as relative values with reference to the elastic modulus of the unheated ECC mixtures.

Figure 5(b) shows the effect of temperature on the residual compressive strength and stiffness of the ECC, where the compressive strength and stiffness are given as relative values, with reference to those of the unheated (control) specimens. As seen in Fig. 5(b), the effect of high temperatures up to 200°C (392°F) on the stiffness and compressive strength of ECC is similar. After initial heating up to 200°C (392°F), both the compressive strength and modulus of elasticity were reduced by approximately 15% of those of unheated control specimens. This decrease may be due to internal cracking, discussed in a previous section. The occurrence of microcracking can be attributed to the dense microstructure of the ECC matrix, which favors steam-pressure buildups, followed by high tensile stresses. The reason for the dense microstructure of the ECC mixture can be attributed to a significantly lower water-cementitious material ratio (*w/cm*), high FA content, and an absence of coarse aggregate. The use of high-volume FA likely resulted in a denser matrix by reducing the pore size and thickness of the transition zone between fibers and the surrounding cementitious matrix.[30] According to Mehta and Monteiro,[31] the existence of microcracks in the transition zone at the interface with coarse aggregate is the primary reason that concrete is more permeable than the corresponding hydrated cement paste and mortar. Also, in general, with everything else being the same, the larger the aggregate size, the higher the local water-cement ratio (*w/c*) in the interfacial transition zone and, consequently, the weaker and more permeable the concrete.

Figure 5(b) shows that as peak temperature increases from room temperature to 400°C (752°F), the compressive strength of ECC drops slightly, followed by a small amount of microcracking on the surface, when compared to ECC specimens after initial heating up to 200°C (392°F). In general, compressive strength can be considered as a constant. The constant compressive strength evident between 200 and 400°C (392 and 752°F), despite significant loss of weight and increase in porosity, is an interesting phenomenon. The increase in porosity is most likely due to the additional porosity and small channels created in the ECC by melting PVA fibers. It is also important to note that despite the increase in total intruded porosity, the average pore diameter of the ECC matrix (coarsening) shows little change up to 400°C (752°F). These results indicate, therefore, that in addition to providing high tensile ductility at normal temperatures, PVA fibers in ECC can also prevent explosive spalling by melting at approximately 230°C (446°F). Water vapor in ECC can then escape through interconnected channels without creating detrimental internal pressure. The plateau in compressive strength between 200 to 400°C (392 and 752°F) may also be linked to the fact that, despite the increase in total intruded porosity, the average pore diameter of ECC matrix (coarsening) shows little change up to 400 °C (752°F).

At 400°C (752°F), the stiffness loss is significant. Dropping to 66% of its original value, the stiffness response is clearly different from the constant compressive strength behavior between 200 and 400°C (392 and 752°F). Heating to 400°C (752°F) generates a relatively insignificant amount of microcracking (Fig. 6) and a significant amount of mass loss. These did not cause any immediate loss of carrying capacity in compression, however, due to the lack of sensitivity of compressive strength to microcracks and moisture loss.[32,33] This conclusion is confirmed by the stronger correlation that mass (or moisture) loss shows with stiffness than with compressive strength, as indicated in Fig. 8.

When the temperature reaches 600°C (1112°F) and above, the compressive strength starts to decrease dramatically. As indicated in Table 5, an average of 53% of the compressive strength of the unheated concrete was retained after exposure to peak temperature of 600°C (1112°F). After exposure to 800°C (1472°F), it was further reduced to 34%. At exposure

temperatures of 600 and 800°C (1112 and 1472°F), the stiffness of ECC also decreased to approximately 35 and 22% of its original value at room temperature, respectively. Microstructural analysis revealed that the rapid degradation of mechanical properties at exposure temperatures up to 600°C (752°F) is most likely due to the physical changes (increase in porosity, main pore radius of ECC matrix, and cracking density) taking place in the matrix. After an exposure temperature of 600°C (1112°F), the main causes of deterioration in compressive strength and stiffness may be attributed to both the physical transformation of the matrix and the chemical transformation of hydration products. When the temperature was raised to 600°C (1112°F), the decomposition of the major hydrate, known as tobermorite (gel), was inevitable,[27] causing severe deterioration in the microstructure of its matrix and the loss of binder property. Disintegration of silica sand may also occur at 800°C (1472°F).[34]

Compared with previous studies dealing with normal concrete[28,35-37] tested under similar conditions, the residual mechanical properties of ECC mixture at 600°C (1112°F) and above remain remarkable, which may be due to the presence of PVA fibers and the high-volume FA. The benefits of PVA fibers have already been discussed in this paper. Recent studies have shown that the addition of FA can also improve the residual compressive strength of cement paste; this improvement is especially significant for exposure temperatures above 400°C (752°F).[32,35,36] Calcium hydroxide (CH) decomposes after exposure to temperatures greater than 400 to 600°C (752 to1112°F),[35] and the rehydration of dissociated CH becomes a detrimental cause of cracking, and is accompanied by a 44% volume increase.[38] Therefore, the reduced CH in ECC matrix containing FA (which occurs due to pozzolanic reaction) may be an additional factor that leads to reduced cracking and improved mechanical properties.[32,36]

CONCLUSIONS

This investigation was carried out to develop data on the effect of elevated temperatures on the mechanical and microstructural properties of ECC. A standard ECC mixture (M45) with an FA/PC ratio of 1.2 was investigated. Mechanical properties (compressive strength, stress-strain relationship, and stiffness) and microstructural properties (via MIP and SEM analyses) of ECC were studied at room temperature and after exposure to peak temperatures up to 800°C (1472°F) for 1 hour. Based on this study, the following conclusions can be drawn:

- For exposure to peak temperatures of 200°C (392°F), a slight reduction (approximately 15%) in compressive strength and stiffness, but no significant changes in microstructure were observed.
- When specimens were exposed to peak temperatures of 200 and 400°C (392 and 752°F), microstructural analysis showed supplementary pores and small channels created in the ECC matrix due to PVA fiber melting. Small hairline cracks were also observed on the surface after specimens had been exposed to 400°C (752°F). Even when the maximum exposure temperature was raised to 400°C (752°F), the strength reductions were as low as 15%.
- After exposure to 600°C (1112°F), the ECC mixture retained approximately 53% its compressive strength, and surface cracking was more significant. The compressive strength of ECC deteriorated even more when the exposure peak temperature was raised to 800°C (1472°F), and the residual strengths were approximately 34% of the values obtained from the unheated control specimens. When compared with specimens exposed to a peak temperature of 600°C (1112°F), the total porosity of ECC did not change after it was subjected to a maximum temperature of 800°C (1472°F), despite the fact that the average pore diameter increased significantly at the same time. For peak temperatures above 400°C (752°F), microstructural analyses revealed that physical change (increase in total intruded porosity, the average pore diameter, and surface cracking) in the ECC matrix is not the only parameter affecting its strength. Other factors such as deterioration of the hydration products and sand are also important determinants of mechanical properties of ECC exposed to 800°C (1472°F).
- Loss of material stiffness occurred much quicker upon exposure to peak temperatures of 400°C (752°F) and above, as compared with the loss of compressive strength.

It can be found by comparing the data given in this paper with published work on normal concrete or fiber-reinforced concrete[26,33-35] that the standard ECC mixture (by retaining more than 35% of its original compressive strength and 22% of its original stiffness capacity after exposure to peak temperatures of 800°C (1472°F) for 1 hour performs similarly to or better than fire-damaged plain concrete with steel and/or polypropylene fibers exposed to similar elevated temperatures. Moreover, explosive spalling was not observed in any ECC specimens. To increase confidence in predicting the behavior of ECC structural members under fire exposure, however, fire tests using realistic fire curves on full-scale members will need to be carried out to obtain realistic and consistent results. The results reported in the present paper provide a preliminary database of ECC material behavior under fire.

ACKNOWLEDGMENTS

The authors gratefully acknowledge the financial assistance of the Scientific and Technical Research Council (TUBITAK) of Turkey provided under Project MAG-108M495, the Natural Sciences and Engineering Research Council (NSERC) of Canada, the Canada Research Chair Program, and the University of Michigan E. B. Wylie Professorship funds.

REFERENCES

1. Li, V. C., "Engineered Cementitious Composites—Tailored Composites through Micromechanical Modeling," *Fiber Reinforced Concrete: Present and the Future*, N. Banthia, A. Bentur, and A. Mufti, eds., Canadian Society for Civil Engineering, Montreal, QC, Canada, 1997, pp. 64-97.

2. Li, V. C., "On Engineered Cementitious Composites (ECC)—A Review of the Material and its Applications," *Journal of Advanced Concrete Technology*, V. 1, No. 3, 2003, pp. 215-230.

3. Sahmaran, M., and Li, V. C., "De-Icing Salt Scaling Resistance of Mechanically Loaded Engineered Cementitious Composites," *Cement and Concrete Research*, V. 37, No. 7, 2007, pp. 1035-1046.

4. Sahmaran, M.; Li, V. C.; and Li, M., "Transport Properties of Engineered Cementitious Composites under Chloride Exposure," *ACI Materials Journal*, V. 104, No. 6, Nov.-Dec. 2007, pp. 604-611.

5. Sahmaran, M., and Li, V. C., "Durability of Mechanically Loaded Engineered Cementitious Composites under High Alkaline Environment," *Cement and Concrete Composites*, V. 30, No. 2, 2008, pp. 72-81.

6. Sahmaran, M.; Li, V. C.; and Andrade, C., "Corrosion Resistance Performance of Steel-Reinforced Engineered Cementitious Composites Beams," *ACI Materials Journal*, V. 105, No. 3, May-June 2008, pp. 243-250.

7. Sahmaran, M., and Li, V. C., "Influence of Microcracking on Water Absorption and Sorptivity of ECC," *Materials and Structures*, V. 42, No. 5, 2009, pp. 593-603.

8. Li, M.; Sahmaran, M.; and Li, V. C., "Effect of Cracking and Healing on Durability of Engineered Cementitious Composites under Marine

Environment," *HPFRCC 5—High Performance Fiber Reinforced Cement Composites*, Stuttgart, Germany, V. 10-13, 2007, pp. 313-322.

9. Sahmaran, M.; Lachemi, M.; and Li, V. C., "Assessing the Durability of Engineered Cementitious Composites under Freezing and Thawing Cycles," *Journal of ASTM International*, V. 6, No. 7, 2009, 13 pp.

10. Lepech, M., and Li, V. C., "Large Scale Processing of Engineered Cementitious Composites," *ACI Materials Journal*, V. 105, No. 4, July-Aug. 2008, pp. 358-366.

11. Kunieda, M., and Rokugo, K., "Recent Progress on HPFRCC in Japan," *Journal of Advanced Concrete Technology*, V. 4, No. 1, 2006, pp. 19-33.

12. Li, V. C.; Lepech, M.; and Li, M., "Field Demonstration of Durable Link Slabs for Jointless Bridge Decks Based on Strain-Hardening Cementitious Composites," Report for Michigan Department of Transportation (DOT) RC-1438, 2005.

13. Li, V. C.; Wang, S.; and Wu, C., "Tensile Strain-Hardening Behavior of PVA-ECC," *ACI Materials Journal*, V. 98, No. 6, Nov.-Dec. 2001, pp. 483-492.

14. Kong, H. J.; Bike, S.; and Li, V. C., "Constitutive Rheological Control to Develop a Self-Consolidating Engineered Cementitious Composite Reinforced with Hydrophilic Poly(vinyl Alcohol) Fibers," *Cement and Concrete Composites*, V. 25, No. 3, 2003, pp. 333-341.

15. Breitenbücker, R., "High Strength Concrete C 105 with Increased Fire Resistance Due to Polypropylene Fibres," F. de Larrad and R. Lacroix, eds., 4th International Symposium on the Utilization of High-Strength/ High-Performance Concrete, Paris, France,1996, pp. 571-577.

16. Sarvaranta, L.; Jarvela, E.; and Mikkola, E., "Fibre Mortar Composites under Thermal Exposure," *Proceedings of 2nd International Symposium on Textile Composites in Building Construction*, Pluralis, ed., Lyon, France, 1992, pp. 47-56.

17. Sarvaranta, L., and Mikkola, E., "Fibre Mortar Composites in Fire Conditions," *Fire and Materials*, V. 18, No. 1, 1994, pp. 45-50.

18. Sarvaranta, L., and Mikkola, E., "Fibre Mortar Composites under Fire Conditions: Effects of Ageing and Moisture Content of Specimens," *Materials and Structures*, V. 27, No. 9, 1994, pp. 532-538.

19. Nishida, A.; Yamazaki, N.; Inoue, H.; Schneider, U.; and Diederichs, U., "Study on the Properties of High-Strength Concrete with Short Polypropylene Fibers for Spalling Resistance," *Proceedings of the Symposium on Concrete Under Severe Environment 2*, K. Sakai, N. Banthia, and O. E. Gjorv, eds.,1995, pp. 1141-1150.

20. Diederichs, U.; Jumppanen, U. M.; and Schneider, U., "High Temperature Properties and Spalling Behaviour of High-Strength Concrete," *4th International Workshop on High Performance Concrete—Characteristics, Material Properties and Structural Performance*, Weimar, Germany, 1995, pp. 219-235.

21. Lennon, T., and Clayton, N., "Fire Tests on High Grade Concrete with Polypropylene Fibres," *BRE Report* 395, 1999.

22. Kalifa, P.; Menneteau, F. D.; Quenard, D., "Spalling and Pore Pressure in HPC at High Temperatures," *Cement and Concrete Research*, V. 30, No. 12, 2000, pp. 1915-1927.

23. Li, V. C.; Wu, C.; Wang, S.; Ogawa, A.; and Saito, T., "Interface Tailoring for Strain-Hardening PVA-ECC," *ACI Materials Journal*, V. 99, No. 5, Sept.-Oct. 2002, pp. 463-472.

24. Mohamedbhai, G. T. G., "Effect of Exposure Time and Rates of Heating and Cooling on Residual Strength of Heated Concrete," *Magazine of Concrete Research*, V. 38, No. 136, 1986, pp. 151-158.

25. Rostasy, R. S.; Weiss, R.; and Wiedemann, G., "Changes of Pore Structure of Cement Mortar Due to Temperatures," *Cement and Concrete Research*, V. 10, No. 2,1980, pp. 157-164.

26. Khoury, G. A., "Compressive Strength of Concrete at High Temperatures: A Reassessment," *Magazine of Concrete Research*, V. 44, No. 161, 1992, pp. 291-309.

27. Khoury, G. A.; Grainger, B. N.; and Sullivan, P. J. E., "Transient Thermal Strain of Concrete: Literature Review, Conditions within Specimen and Behavior of Individual Constituents," *Magazine of Concrete Research*, V. 37, No. 132, 1985, pp. 131-144.

28. Luo, X.; Sun, W.; and Chan, S. Y. N., "Effect of Heating and Cooling Regimes on Residual Strength and Microstructure of Normal Strength and High-Performance Concrete," *Cement and Concrete Research*, V. 30, No. 3, 2000, pp. 379-383.

29. Lam, L.; Wong, Y. L.; and Poon, C. S., "Effect of Fly Ash and Silica Fume on Compressive and Fracture Behaviors of Concrete," *Cement and Concrete Research*, V. 28, No. 2, 1998, pp. 271-280.

30. Kuroda, M.; Watanabe, T.; and Terashi, N., "Increase of Bond Strength at Interfacial Transition Zone by the Use of Fly Ash," *Cement Concrete Research*, V. 30, No. 2, 2000, pp. 253-258.

31. Mehta, P. K., and Monteiro, P. J. M., *Concrete: Structure, Properties, and Materials*, third edition, McGraw Hill Companies, Inc., New York, 2006, 659 pp.

32. Xu, Y.; Wong, Y. L.; Poon, C. S.; and Anson, M., "Influence of PFA on Cracking of Concrete and Cement Paste after Exposure to High Temperatures," *Cement and Concrete Research*, V. 33, No. 12, 2003, pp. 2009-2016.

33. Wu, B.; Su, X. P.; Li, U.; and Yuan, J., "Effect of High Temperature on Residual Mechanical Properties of Confined and Unconfined High-Strength Concrete," *ACI Materials Journal*, V. 99, No. 4, July-Aug. 2002, pp. 399-407.

34. Bažant, Z. P., and Kaplan, M. F., *Concrete at High Temperatures: Material Properties and Mathematical Models*, Longman Group, UK, 1996, 424 pp.

35. Dias, W. P. S.; Khoury, G. A.; and Sullivan, P. J. E., "Mechanical Properties of Hardened Cement Paste Exposed to Temperatures Up to 700°C," *ACI Materials Journal*, V. 87, No. 2, Mar.-Apr. 1990, pp. 160-166.

36. Xu, Y.; Wong, Y. L.; Poon, C. S.; and Anson, M., "Impact of High Temperature on PFA Concrete," *Cement and Concrete Research*, V. 31, No. 7, 2001, pp. 1065-1073.

37. Taylor, H. F. W., *The Chemistry of Cements*, Academic Press, London, UK, 1964, 480 pp.

38. Petzold, A., and Rohr, M., *Concrete for High Temperatures*, Maclaren and Sons, London, UK, 1970, 232 pp.